

## Original Article

# Radiosynthesis and preclinical evaluations of [<sup>18</sup>F]AIF-RESCA-5F7 as a novel molecular probe for HER2 tumor imaging

Ruhua Tian<sup>1\*</sup>, Jinping Kong<sup>1\*</sup>, Yingfang He<sup>2</sup>, Guoqiang Xu<sup>1</sup>, Tengxiang Chen<sup>1</sup>, Junbin Han<sup>1,2</sup>

<sup>1</sup>Department of Physiology, School of Basic Medicine, Guizhou Medical University, Guiyang 550009, Guizhou, China; <sup>2</sup>Institute of Radiation Medicine, Fudan University, No. 2094 Xietu Road, Shanghai 200032, China. \*Equal contributors.

Received March 5, 2024; Accepted May 15, 2024; Epub June 15, 2024; Published June 30, 2024

**Abstract:** HER2 overexpression is associated with various tumor types and prompted the development of targeted therapies. Previously, *iso*-[<sup>211</sup>At]SGMAB-5F7 was developed as a HER2-targeted alpha therapy agent, demonstrating promising therapeutic efficacy in the pre-clinical stage. Aiming for an <sup>18</sup>F-labeled tracer for companion diagnostics in clinical translation, we employed the Al<sup>18</sup>F-RESCA strategy in our current work and investigated whether [<sup>18</sup>F]AIF-RESCA-5F7 could visualize HER2 expression *in vivo*. [<sup>18</sup>F]AIF-RESCA-5F7 was attained with high radiochemical purity (> 99%) and molar activity in the range of 16.5 ± 8.8 GBq/μmol (n = 8). Compared to previously reported radiotracers that contained 5F7 as the HER2-targeting carrier and fluorine-18 as the positron-emitting isotope, the radiosynthesis was simplified to one single step within 30 min. The dissociation constant of [<sup>18</sup>F]AIF-RESCA-5F7 was determined as 3.3 nM *via* saturation binding assay using SKOV3 ovarian carcinoma cells. Tumor uptake of the novel tracer in Balb/c nude mice bearing SKOV3 xenografts was 4.69 ± 1.51, 3.34 ± 0.82 and 3.77 ± 0.99 %ID/g at 1, 2, and 4 h post-injection. Even though high retention of radioactivity was seen in the kidneys, micro-PET/CT imaging of [<sup>18</sup>F]AIF-RESCA-5F7 delineated the tumor up to 4 h post-injection with minimal activity in the gallbladder, intestines, and bone. This study suggests that [<sup>18</sup>F]AIF-RESCA-5F7 is a promising HER2 PET radiotracer with an eased radiolabeling method. Whether [<sup>18</sup>F]AIF-RESCA-5F7 could work as a companion diagnostic agent to assist in patient stratification and treatment monitoring of *iso*-[<sup>211</sup>At]SGMAB-5F7 warrants further investigation.

**Keywords:** HER2 overexpression, PET, VHH, Al<sup>18</sup>F-RESCA method, preclinical evaluations

## Introduction

Receptor tyrosine-protein kinase erbB-2, also called HER2, is a member of the epidermal growth factor receptor family of receptor tyrosine kinases. Overexpression of HER2 promotes cellular proliferation and tumorigenesis *via* the autophosphorylation of tyrosine residues within the cytoplasmic domain of the heterodimer [1]. Anti-HER2 monoclonal antibody, such as trastuzumab and pertuzumab, was approved for the treatment against HER2-positive breast cancer. Besides, HER2-targeted therapies are tested in clinics for patients with other solid tumors containing HER2 overexpression and/or amplification [2]. With patient stratification and treatment monitoring goals, the development of radioligands has gained substantial interest in non-invasively visualizing HER2 *via* positron emission tomography (PET) [3-5].

Single-domain antibody fragments (sdAb), or VHH or nanobody, are the smallest natural antigen-binding fragments derived from Camelids [6]. The low molecular weight of 12-15 kDa allows nanobodies to clear faster from the blood than the intact antibody and thus makes them ideal for labeling with fluorine-18 for PET imaging [7, 8]. 5F7, an anti-HER2 sdAb, was previously conjugated with various prosthetic agents for <sup>18</sup>F-labeling, as shown in **Figure 1A** [9-11]. Generally, these molecular probes exhibited excellent PET tumor imaging in athymic mice bearing SKOV3 or BT474 xenograft with low background

activity levels in normal tissues, except the bladder or/and the kidneys. However, their radiosyntheses usually request at least two steps, including the radiofluorination of a prosthetic agent and subsequent reaction with lysine residues of 5F7 in borate buffer or trans-cyclooctene (TCO) functionalized 5F7 *via* the inverse electron-demand Diels-Alder reaction. The total synthesis time is usually long with a low-to-moderate radiochemical yield (RCY), up to 20% decay-corrected RCY in the case of [<sup>18</sup>F]FN-GK-5F7. Most recently, *iso*-[<sup>211</sup>At]SGMAB-5F7 (**Figure 1B**) was reported as a promising agent for targeted alpha therapy of HER2-expressing cancers in the preclinical stage [12]. Thus, a simplified <sup>18</sup>F-labeling 5F7 is highly attractive for companion diagnostics, particularly in future clinical translation.

The Al<sup>18</sup>F labeling method has become convenient for attaining <sup>18</sup>F-labeled biomolecules [13]. It allows radiofluorination with a one-step procedure *via* forming aluminum monofluoride ([Al<sup>18</sup>F]<sup>2+</sup>), which is trapped in the chelator-conjugated peptide or protein. Conventional Al<sup>18</sup>F-strategy using macrocyclic chelators, such as 1,4,7-triazacyclononane-1,4,7-triacetic acid (NOTA) and 1,4,7-triazacyclononane-1,4-diacetic acid (NODA), generally requests high temperature (> 100°C). Such harsh conditions are not compatible with heat-sensitive biomolecules. Recently, Cleeren *et al.* published a new Al<sup>18</sup>F-chelation employing a tetrafluorophenyl ester derivative of the restrained complexing agent [(±)-H3RESCA-TFP], an acy-

# Novel $^{18}\text{F}$ -radiolabeling molecular probe for HER2 tumor imaging

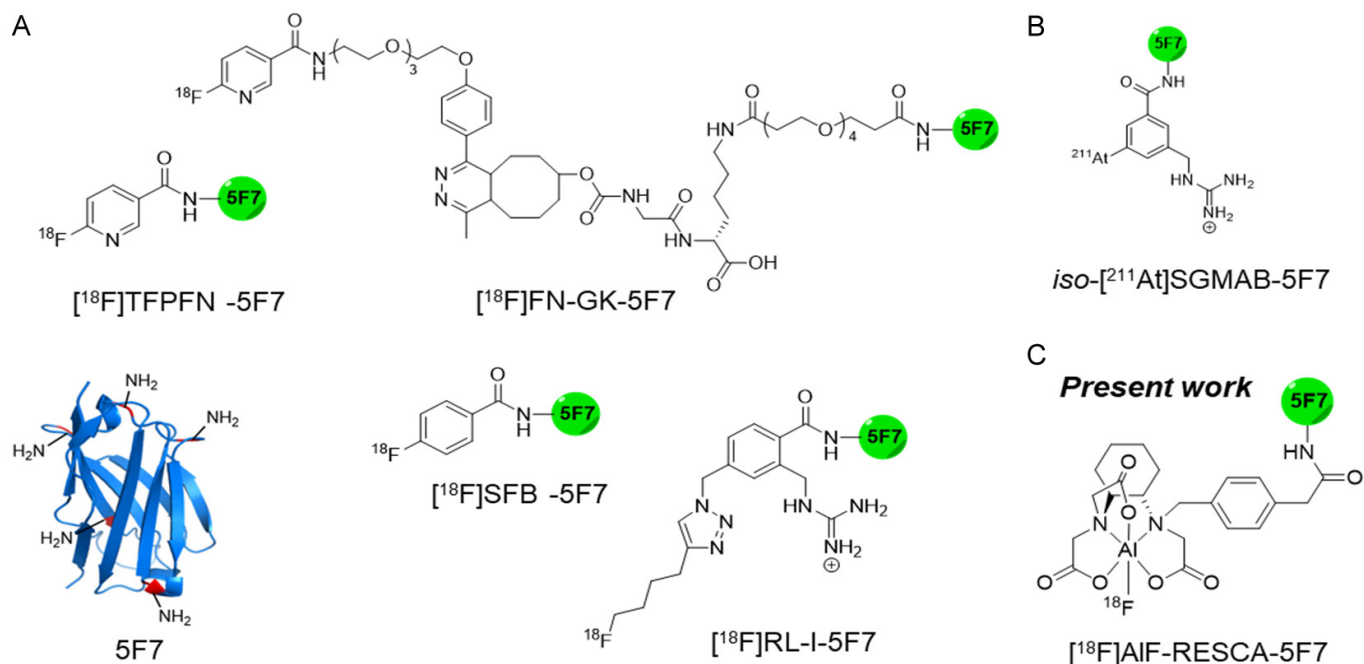


**Figure 1.** A.  $^{18}\text{F}$ -radiolabeling 5F7 via a variety of prosthetic agents; B. Chemical structures of *iso*- $^{211}\text{At}$ SGMAB-5F7; C.  $^{18}\text{F}$ AIF-RESCA-5F7 labeled and evaluated in present work.

clic pentadentate ligand with an  $\text{N}_2\text{O}_3$  coordinative set [14]. This approach achieved efficient radiolabeling at room temperature, and the resulting  $\text{Al}^{18}\text{F}$ -complex demonstrated high *in vivo* stability in preclinical and clinical studies [15, 16]. In the present work, we report on the radiosynthesis of  $^{18}\text{F}$ AIF-RESCA-5F7 (Figure 1C) to simplify the previously reported radiofluorination approach. The *in vitro* stability of the tracer was investigated in the final formulation. Biological evaluations were conducted to investigate its kinetic profile, including cellular retention and internalization, biodistribution, and PET imaging.

## Materials and methods

### General

All reagents were obtained from commercially available resources and used without further purification except where noted. The human ovarian cancer cell line SKOV3 was purchased from the National Collection of Authenticated Cell Cultures (Shanghai, China). The cells were routinely grown in MCCOY'S 5A medium supplemented with 10% fetal bovine serum (FBS) and 1% penicillin and streptomycin in an atmosphere containing 5%  $\text{CO}_2$  at 37°C. All animal experiments were approved by the Institutional Animal Care and Use Committee of Fudan University (202308037S).

### Preparation of ( $\pm$ )-H3RESCA-5F7 conjugates

The anti-HER2 sdAb 5F7 was kindly provided by Zentara Therapeutics (Shanghai, China). Adjusting pH to 8.5 using 0.05 M sodium carbonate-bicarbonate buffer, an excessive amount of ( $\pm$ )-H3RESCA-TFP (10 eq) with the acyclic chelator was added and coupled to the 5F7. The reaction

was shaken at room temperature for 2 h. Afterward, the mixture was loaded to a pre-conditioned PD-10 column (GE Healthcare), and 0.1 M ammonium acetate buffer (pH 4.4-4.6) was employed as an eluent. The concentration in each fraction was measured with Nanodrop (Mettler Toledo GmbH, UV5NANO), and the molar extinction coefficient for 5F7 was set to 21555  $\text{M}^{-1}\text{cm}^{-1}$  [17]. Peak fractions were combined and stored at -20°C until the day of radiolabeling.

### Radiochemistry

The no-carrier-added  $^{18}\text{F}$ fluoride was obtained by the bombardment of 98% enriched  $^{18}\text{O}$ -water via  $^{18}\text{O}(\text{p},\text{n})^{18}\text{F}$  nuclear reaction with 11 MeV protons in a RDS 111 cyclotron (Siemens, Germany). An aqueous solution containing  $^{18}\text{F}\text{F}^-$  was trapped on a QMA cartridge (Sep-Pak Accell Plus QMA Light cartridge). The cartridge was rinsed with 5 mL of deionized water. The concentrated  $^{18}\text{F}\text{F}^-$  was eluted with 0.9% NaCl (wt/vol) and collected in the LoBind Eppendorf tube. Pipette 10  $\mu\text{L}$  of 2 mM  $\text{AlCl}_3$  into an aliquot of the eluted  $^{18}\text{F}\text{F}^-$  (> 1.1 GBq, 100  $\mu\text{L}$ ), and the resulting solution was incubated at room temperature for 5 min before the addition of ( $\pm$ )-H3RESCA-5F7 (200  $\mu\text{g}$ , 16 nmol). After incubation at room temperature for 10 min, the mixture was purified using a PD-10 column with saline as an eluent. The radiochemical purity (RCP) of  $^{18}\text{F}$ AIF-RESCA-5F7 was determined by radio-TLC (Mini-Scan, Eckert & Ziegler Radiopharma, Inc. MS-100) using 0.01 M phosphate-buffered saline (PBS) buffer as the mobile phase. The size exclusion-chromatography (SEC) on UltiMate™ 3000 HPLC systems equipped with a UV detector and a radioactive detector (Gabi Nova, Mid Energy, 2 × 2" NaI-PMT) using TSKgel UP-SW2000 column (2  $\mu\text{m}$ , 4.6

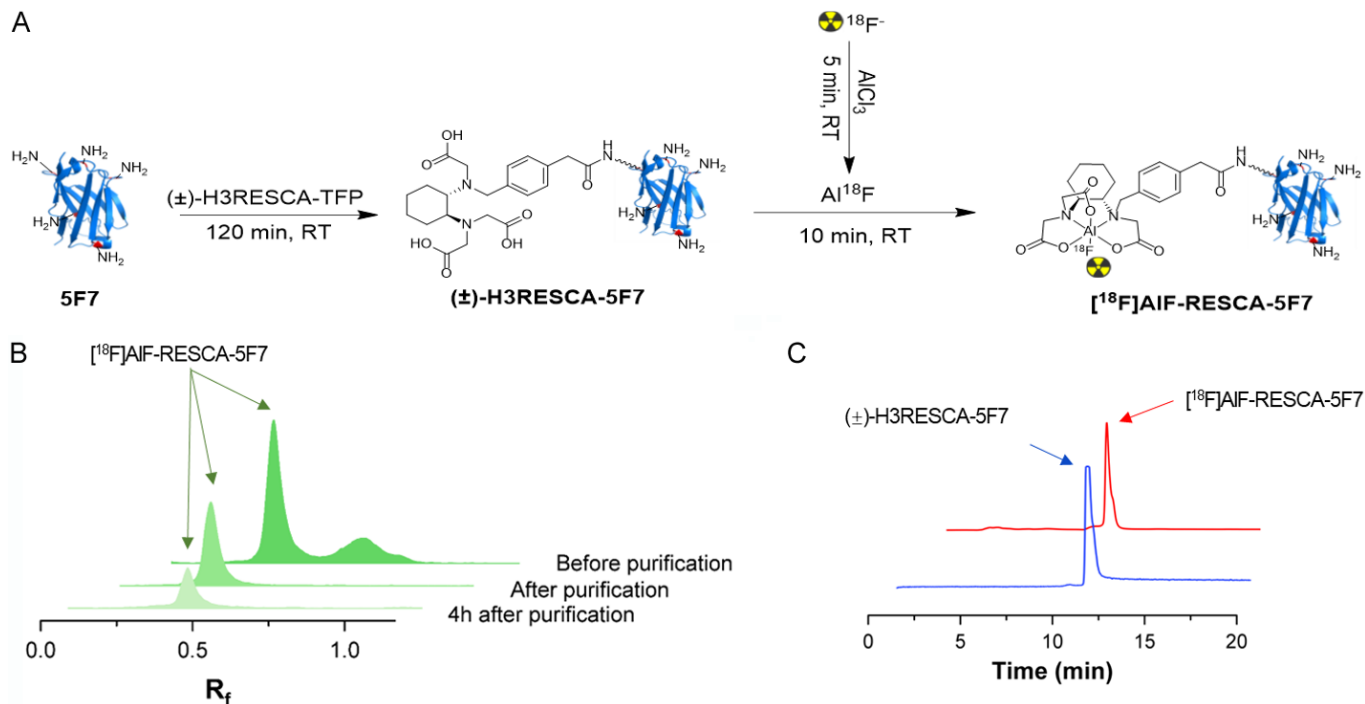


**Figure 2.** A. Radiosynthesis of  $[^{18}\text{F}]\text{AIF-RESCA-5F7}$ ; B. Radio-thin-layer chromatograms of reaction mixture,  $[^{18}\text{F}]\text{AIF-RESCA-5F7}$  and  $[^{18}\text{F}]\text{AIF-RESCA-5F7}$  after 4 h storage at room temperature; C. Co-injection of  $[^{18}\text{F}]\text{AIF-RESCA-5F7}$  and  $(\pm)\text{-H3RESCA-5F7}$  using size exclusion chromatography.

mm  $\times$  30 cm, Tosoh Bioscience LLC, King of Prussia, PA). 0.01 M PBS containing 3%  $\text{NaN}_3$  was employed as the eluent with a flow of 0.35 mL/min under the wavelength of 280 nm. The radiochemical yield (RCY) was determined as the ratio of the  $[^{18}\text{F}]\text{AIF-RESCA-5F7}$  to the total radioactivity in the aliquot with decay correction.

#### *In vitro stability*

The *in vitro* stability of  $[^{18}\text{F}]\text{AIF-RESCA-5F7}$  complexes was investigated as previously reported [18]. Briefly,  $[^{18}\text{F}]\text{AIF-RESCA-5F7}$  in the final formulation was stored at room temperature for 4 h and analyzed by SEC using 0.01 M PBS buffer as the mobile phase.

#### *Determination of dissociation constant ( $K_d$ )*

The 24-well plate was seeded with approx.  $1 \times 10^5$  cells per well 24 h before the experiment. On the experimental day, the monolayers were rinsed twice with ice-cold PBS (pH = 7.4).  $[^{18}\text{F}]\text{AIF-RESCA-5F7}$  ( $\sim 20$  GBq/ $\mu\text{mol}$ ) was prepared in cold PBS with concentrations. After 2 h incubation at  $4^\circ\text{C}$ , the medium was removed. The plate was then washed twice with cold PBS and lysed with 300  $\mu\text{L}$  of 1 M NaOH for 20 min. The lysates were collected and measured in an automatic Gamma Counter (Wizard<sup>®</sup> 2470, PerkinElmer, USA). Nonspecific binding was defined by co-incubation of 23  $\mu\text{M}$  trastuzumab. The nonlinear regression was fitted in GraphPad Prism Software (One-site - Total and nonspecific binding, version 9.5.0) to calculate the  $K_d$ .

#### *Cellular retention and internalization*

The assay was conducted in triplet, as previously reported [19]. Briefly, the harvested cells were seeded in 6-well plates with several  $1 \times 10^6$  cells/well and incubated with 3 mL MCCOY'S 5A medium supplemented with 10% fetal bovine serum (FBS) and 1% penicillin and streptomycin 24 h before the experiment. On the experimental day, cells in each well were incubated with  $[^{18}\text{F}]\text{AIF-RESCA-5F7}$  (0.296 MBq) dissolved in MCCOY'S 5A medium at  $4^\circ\text{C}$  for 0.5 h. After washing with PBS, the plate was replenished with fresh medium and incubated at  $37^\circ\text{C}$ . At 1, 2, and 4 h of incubation, the medium was removed, and the cells were quickly washed twice with ice-cold PBS buffer (pH = 7.4) containing 0.2% bovine serum albumin (BSA). The membrane-bound radioactivity was dissociated using ice-cold 0.2 M glycine buffer (0.15 M NaCl, 4 M urea, pH = 2) [20]. The remaining activity was considered internalized. The lysates were collected by incubating with 1 M NaOH for 20 min at room temperature, and the radioactivity was measured with an automatic Gamma Counter (Wizard<sup>®</sup> 2470, PerkinElmer, USA). The results were expressed as the percentages of initially bound activity.

#### *Biodistribution*

A group of four Balb/c mice bearing SKOV3 xenografts received  $[^{18}\text{F}]\text{AIF-RESCA-5F7}$  (2.95 MBq, 3.9  $\mu\text{g}$ ) in 100  $\mu\text{L}$  saline *via* the tail vein. The animal was sacrificed by decapitation under anesthesia at 1, 2, and 4 h post-injec-

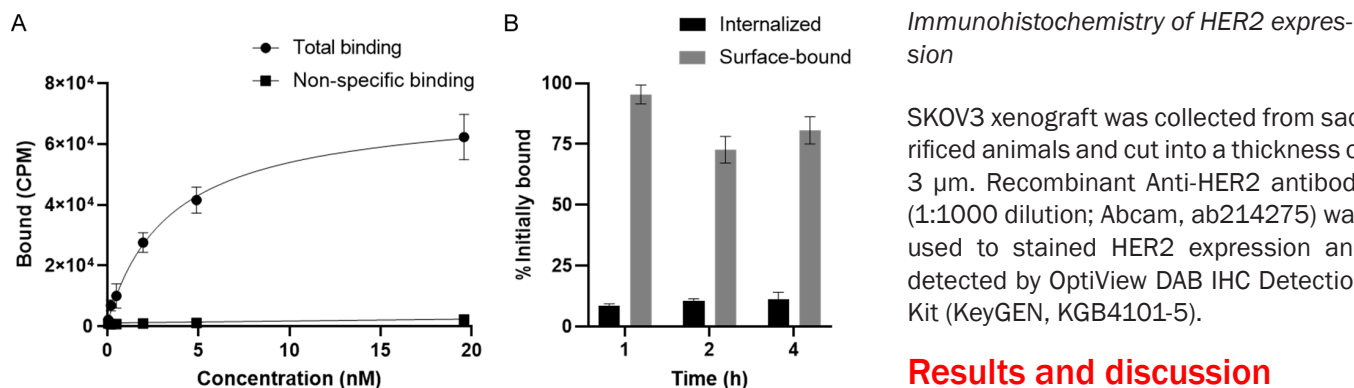


**Figure 3.** A. Saturation binding curves of [ $^{18}\text{F}$ ]AIF-RESCA-5F7 in the SKOV3 cells to determine  $K_d$  value. B. Cellular internalization of [ $^{18}\text{F}$ ]AIF-RESCA-5F7 in SKOV3 cells. The results are presented as surface-bound and internalized fractions of the radioactivity initially bound to the cells after 1, 2 and 4 h incubation at 4 °C.

**Table 1.** Biodistribution of [ $^{18}\text{F}$ ]AIF-RESCA-5F7 in Balb/c mice bearing SKOV3 xenografts<sup>a</sup>

| Organ                        | 1 h          | 2 h          | 4 h          |
|------------------------------|--------------|--------------|--------------|
| Heart                        | 0.34 ± 0.04  | 0.14 ± 0.01  | 0.11 ± 0.01  |
| Liver                        | 1.06 ± 0.19  | 0.75 ± 0.12  | 0.47 ± 0.09  |
| Spleen                       | 0.44 ± 0.18  | 0.22 ± 0.01  | 0.20 ± 0.08  |
| Lung                         | 0.79 ± 0.17  | 0.34 ± 0.03  | 0.25 ± 0.01  |
| Kidney                       | 23.29 ± 6.67 | 15.29 ± 4.16 | 8.53 ± 1.76  |
| Bone                         | 2.61 ± 0.62  | 2.43 ± 0.09  | 2.98 ± 0.47  |
| Stomach <sup>b</sup>         | 0.06 ± 0.01  | 0.02 ± 0.003 | 0.02 ± 0.003 |
| Muscle                       | 0.38 ± 0.17  | 0.12 ± 0.03  | 0.29 ± 0.26  |
| Small Intestine <sup>b</sup> | 0.07 ± 0.01  | 0.04 ± 0.01  | 0.15 ± 0.005 |
| Tumor                        | 4.69 ± 1.51  | 3.34 ± 0.82  | 3.77 ± 0.99  |
| Blood                        | 0.68 ± 0.43  | 0.52 ± 0.27  | 0.09 ± 0.02  |

<sup>a</sup>Data are means of %ID/g of tissue ± SD (n = 4). <sup>b</sup>%ID/organ.

tion, and the organs of interest, including blood, brain, heart, liver, spleen, lungs, kidney, muscle, bone, and tumor, were dissected, weighed and counted in an automatic Gamma Counter (Wizard<sup>®</sup> 2470, PerkinElmer, USA).

### PET imaging

[ $^{18}\text{F}$ ]AIF-RESCA-5F7 (3.07 MBq, 3.2 μg) was intravenously injected into SKOV3 xenograft tumor-bearing mice (n = 3). The experiment used the Inveon microPET-CT scanner (Siemens Inc., The United States). At 1, 2, and 4 h post-injection, the animal was anesthetized using 2-3% isoflurane with an isoflurane vaporizer (Molecular Imaging Products Company, United States), and static PET/CT imaging was obtained for 15 min using a procedure previously described [21]. 5F7 (80 mg/kg, formulated in PBS buffer) was co-injected with the radiotracer for blocking studies. The data was reconstructed using the ordered subsets expectation maximization 3D algorithm (OSEM3D), reviewed in the Inveon Research Workplace (IRW) software (Siemens), and analyzed using PMOD software (version 4.401, PMOD Technologies Ltd., Zurich, Switzerland).

## Results and discussion

### Radiochemistry

The preparation of (±)-H3RESCA-5F7 and the radiosynthesis of [ $^{18}\text{F}$ ]AIF-RESCA-5F7 are presented in **Figure 2A**. 10-fold molar excess of (±)-H3RESCA-TFP was coupled to 5F7, and the mixture was purified by PD-10 column to obtain (±)-H3RESCA-5F7. On the experimental day, the RESCA-conjugated 5F7 reacted with an aqueous solution of the Al $^{18}\text{F}$  complex. [ $^{18}\text{F}$ ]AIF-RESCA-5F7 was obtained in 20% decay-corrected radiochemical yield (RCY), and the total synthesis time was around 30 min. The radiochemical purity was above 95% as determined by radio-thin-layer chromatography (**Figure 2B**) with a molar activity in the range of 16.5 ± 8.8 GBq/μmol (n = 8). As depicted in **Figure 2C**, co-injection with (±)-H3RESCA-5F7 confirmed the identity of the tracer, and the product in the final formulation was stable after 4 h storage at room temperature. Compared to those of [ $^{18}\text{F}$ ]TFPFN (Two-step with decay-corrected RCY of 4.0 ± 2.0% in 95 min) and [ $^{18}\text{F}$ ]FN-GK-5F7 (Two-step with decay-corrected 20.0 ± 3.0% in 90 min) [10, 11], the  $^{18}\text{F}$ -radiolabeling of [ $^{18}\text{F}$ ]AIF-RESCA-5F7 was completed in one-step within 30 min and provided the desired product with moderate molar activity and high radiochemical purity.

### Cellular assays

The  $K_d$  value of [ $^{18}\text{F}$ ]AIF-RESCA-5F7 was determined as 3.3 nM *via* saturation binding assay using HER2-positive SKOV3 ovarian carcinoma cells (95% confidence intervals [CIs] of 2.5-4.4 nM), as shown in **Figure 3A**. This is similar to those reported for [ $^{18}\text{F}$ ]TFPFN (2.7 nM) and [ $^{18}\text{F}$ ]FN-GK-5F7 (5.4 nM) [10, 11]. After 0.5 h incubation at 4 °C, the plate was washed with PBS, and the remaining radioactivity was considered as initially bound activity. The intracellular uptakes of [ $^{18}\text{F}$ ]AIF-RESCA-5F7 were measured as 9%, 11%, and 11% after incubating the plate 1, 2, and 4 h at 37 °C, respectively. As shown in **Figure 3B**, most of the radiotracer bound to HER2 targets at the surface of the cells. The total cell-bound activity (surface-bound plus internalized) remained above 80% throughout the experiment, suggesting the long retention time of the tracer on the targets.



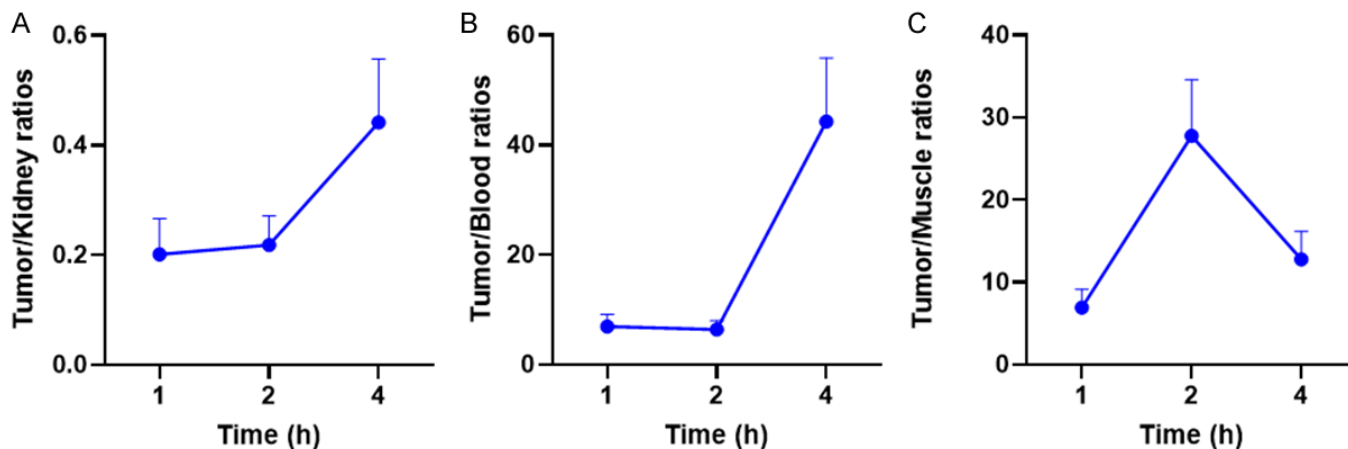


**Figure 4.** Tumor-to-kidney (A), tumor-to-blood (B), tumor-to-muscle (C) ratios after administration of [ $^{18}\text{F}$ ]AIF-RESCA-5F7 in Balb/c mice with subcutaneous SKOV3 xenografts.

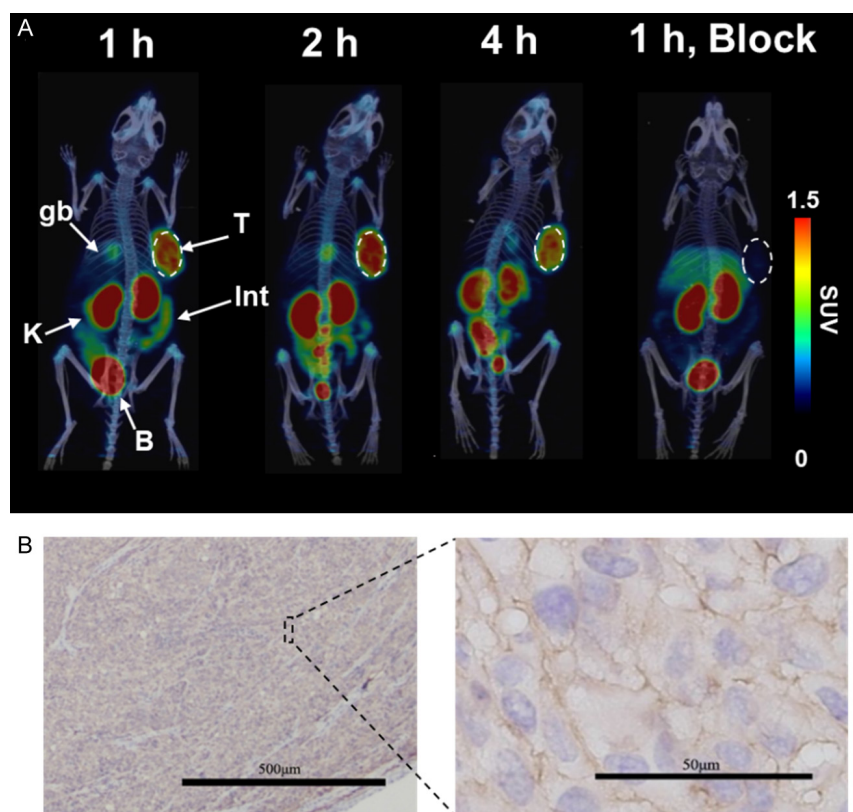


**Figure 5.** A. Representative maximum intensity projection images obtained from microPET/CT imaging of a mouse bearing SKOV3 xenograft at 1, 2, and 4 h post-injection of [ $^{18}\text{F}$ ]AIF-RESCA-5F7 and blocking study at 1 h with a 500-fold molar excess of cold 5F7. T, tumor; GB, gallbladder; K, kidney; Int, intestine; B, bladder. B. HER2 immunohistochemical staining for SKOV3 xenograft.

### Biodistribution

Encouraged by the promising results *in vitro*, biodistribution was carried out using nude mice bearing SKOV3 xenografts. The results were expressed as the percentage of normalized injected dose per gram tissue (%ID/g) and summarized in **Table 1**. At 1 h post-injection, tumor uptake of [ $^{18}\text{F}$ ]AIF-RESCA-5F7 ( $4.69 \pm 1.51$  %ID/g) was similar to [ $^{18}\text{F}$ ]FN-GK-5F7 ( $3.71 \pm 1.51$  %ID/g) in the previ-

ous report. Afterward, the tumor radioactivity accumulation remained at  $3.34 \pm 0.82$  %ID/g and  $3.77 \pm 0.99$  %ID/g at 2 and 4 h post-injection, respectively [11]. Consistent with previous reports, high levels of radioactivity were found in the kidneys due to metabolism. 63% of kidney radioactivity accumulation washed out at 4 h post-injection, leading to an increased tumor-to-kidney ratio (**Figure 4A**). Similarly, at 4 h post-injection, the radioactive uptake in the blood reduced to  $0.09 \pm 0.02$  %ID/g and contributed to the high tumor-to-blood ratio (~44-fold, **Figure 4B**). As shown in **Figure 4C**, the maximal tumor-to-muscle ratio reached 28-fold after 2 h administration of [ $^{18}\text{F}$ ]AIF-RESCA-5F7. The novel tracer demonstrated similar tumor uptake as previously shown by [ $^{18}\text{F}$ ]FN-GK-5F7 in nude mice bearing SKOV3 xenografts. However, the clearance rate of the radioactivity from the kidney was significantly slower. This could be explained by the renal brush border enzyme-cleavable linker in [ $^{18}\text{F}$ ]FN-GK-5F7 [11]. The radioactivity accumulated in the bone was moderate overtime ( $< 3$  %ID/g at 4 h post-injection), which is similar to that reported for [ $^{18}\text{F}$ ]AIF-RESCA-MIRC213 ( $2.95 \pm 0.75$  %ID/g) [16] and lower than [ $^{18}\text{F}$ ]AIF-RESCA-IL2 ( $3.9 \pm 1.2$  %ID/g) [22] in Balb/C mice.

### MicroPET/CT imaging

We further evaluated [ $^{18}\text{F}$ ]AIF-RESCA-5F7 *in vivo* by microPET/CT imaging. Representative maximum intensity projection (MIP) microPET/CT images from a Balb/c mouse bearing SKOV3 xenograft are shown in **Figure 5A**. Early to 1 h post-injection, the tracer delineated the tumor in the animal model, and the tumor uptakes calculated from maximal standardized uptake values were  $1.4 \pm 0.1$ ,

1.3 ± 0.2, and 1.3 ± 0.01 at 1, 2, and 4 h post-injection of [<sup>18</sup>F]AIF-RESCA-5F7, respectively. Co-injection with a 500-fold molar excess of 5F7 significantly reduced the radioactivity accumulated in the SKOV3 xenograft, confirming the specificity of [<sup>18</sup>F]AIF-RESCA-5F7 *in vivo*. The slice cut from the SKOV3 xenograft was then confirmed to be HER2-antigen positive using immunohistochemical staining, as shown in **Figure 5B**. Consistent with results from *ex vivo* biodistribution, the kidney radioactivity accumulation slowly washed out over time, and the tumor-to-kidney ratio reached maximal at 4 h post-injection. In comparison with the PET images from [<sup>18</sup>F]TFPFN [10], we didn't observe profound radioactivity accumulated in the intestine. This may be explained by the difference between the radiolabeling prosthetic agents, which results in different metabolites with various lipophilicity.

## Conclusion

Owing to the novel Al<sup>18</sup>F-RESCA method, we simplified the radiofluorination of 5F7 and prepared [<sup>18</sup>F]AIF-RESCA-5F7 with one-step production. The total synthesis time was shortened to 30 min, and the tracer was attained with high radiochemical purity and molar activity qualified for *in vitro/in vivo* biological evaluations. Saturation binding assay using SKOV3 ovarian carcinoma cells suggests that the novel tracer maintained a high affinity towards HER2. The long retention time of [<sup>18</sup>F]AIF-RESCA-5F7 in the target sites was proved sequentially by *in vitro* cellular assay, *ex vivo* biodistribution, and *in vivo* microPET/CT imaging. In Balb/c nude mice bearing SKOV3 xenografts, [<sup>18</sup>F]AIF-RESCA-5F7 exhibited high tumor-to-blood ratios early to 1 h post-injection, and HER2-positive tumor xenografts were visualized. While the radioactivity in kidneys showed moderate clearance, no severe defluorination was observed from PET images. Our study developed [<sup>18</sup>F]AIF-RESCA-5F7 as a novel molecular probe for HER2 tumor imaging. Its simple radiosynthesis and capacity to map HER2 *in vivo* provide a valuable tool for targeted alpha therapy using 5F7 as a HER2-specific carrier.

## Acknowledgements

We are grateful to the National Natural Science Foundation of China (NSFC 22171050, 82302270) and the Shanghai Municipal Health Commission (GWV-11.1-40). The project is sponsored by the Shanghai Pujiang Program (23PJ1401500).

## Disclosure of conflict of interest

None.

**Address correspondence to:** Tengxiang Chen and Junbin Han, Department of Physiology, School of Basic Medicine, Guizhou Medical University, Guiyang 550009, Guizhou, China. E-mail: txch@gmc.edu.cn (TXC); jhanoa@fudan.edu.cn (JBH)

## References

[1] Yarden Y and Sliwkowski MX. Untangling the ErbB signaling network. *Nat Rev Mol Cell Biol* 2001; 2: 127-137.

- [2] Oh DY and Bang YJ. HER2-targeted therapies - a role beyond breast cancer. *Nat Rev Clin Oncol* 2020; 17: 33-48.
- [3] Ge S, Li J, Yu Y, Chen Z, Yang Y, Zhu L, Sang S and Deng S. Review: radionuclide molecular imaging targeting HER2 in breast cancer with a focus on molecular probes into clinical trials and small peptides. *Molecules* 2021; 26: 6482.
- [4] Miladinova D. Molecular imaging of HER2 receptor: targeting HER2 for imaging and therapy in nuclear medicine. *Front Mol Biosci* 2023; 10: 1144817.
- [5] McGale J, Khurana S, Huang A, Roa T, Yeh R, Shirini D, Doshi P, Nakhla A, Bebawy M, Khalil D, Lotfalla A, Higgins H, Gulati A, Girard A, Bidard FC, Champion L, Duong P, Derle L and Seban RD. PET/CT and SPECT/CT imaging of HER2-positive breast cancer. *J Clin Med* 2023; 12: 4882.
- [6] Schumacher D, Helma J, Schneider AFL, Leonhardt H and Hackenberger CPR. Nanobodies: chemical functionalization strategies and intracellular applications. *Angew Chem Int Ed Engl* 2018; 57: 2314-2333.
- [7] Shen Z, Sang Z and Shi Y. Nanobodies as a powerful platform for biomedicine. *Trends Mol Med* 2022; 28: 1006-1007.
- [8] Bao G, Tang M, Zhao J and Zhu X. Nanobody: a promising toolkit for molecular imaging and disease therapy. *EJNMMI Res* 2021; 11: 6.
- [9] Vaidyanathan G, McDougald D, Choi J, Koumariou E, Weitzel D, Osada T, Lyerly HK and Zalutsky MR. Preclinical evaluation of <sup>18</sup>F-labeled anti-HER2 nanobody conjugates for imaging HER2 receptor expression by immuno-PET. *J Nucl Med* 2016; 57: 967-973.
- [10] Zhou Z, McDougald D, Devoogdt N, Zalutsky MR and Vaidyanathan G. Labeling single domain antibody fragments with fluorine-18 using 2,3,5,6-tetrafluorophenyl 6-[<sup>18</sup>F]fluoronicotinate resulting in high tumor-to-kidney ratios. *Mol Pharm* 2019; 16: 214-226.
- [11] Zhou Z, Zalutsky MR and Vaidyanathan G. Labeling a TCO-functionalized single domain antibody fragment with <sup>18</sup>F via inverse electron demand Diels Alder cycloaddition using a fluoronicotinyl moiety-bearing tetrazine derivative. *Bioorg Med Chem* 2020; 28: 115634.
- [12] Feng Y, Meshaw R, Zhao XG, Jannetti S, Vaidyanathan G and Zalutsky MR. Effective treatment of human breast carcinoma xenografts with single-dose <sup>211</sup>at-labeled anti-HER2 single-domain antibody fragment. *J Nucl Med* 2023; 64: 124-130.
- [13] Archibald SJ and Allott L. The aluminium-<sup>18</sup>F]fluoride revolution: simple radiochemistry with a big impact for radiolabelled biomolecules. *EJNMMI Radiopharm Chem* 2021; 6: 30.
- [14] Cleeren F, Lecina J, Bridoux J, Devoogdt N, Tshibangu T, Xavier C and Bormans G. Direct fluorine-18 labeling of heat-sensitive biomolecules for positron emission tomography imaging using the Al<sup>18</sup>F-RESCA method. *Nat Protoc* 2018; 13: 2330-2347.
- [15] Cleeren F, Lecina J, Ahamed M, Raes G, Devoogdt N, Cavelliers V, McQuade P, Rubins DJ, Li W, Verbruggen A, Xavier C and Bormans G. Al<sup>18</sup>F-labeling of heat-sensitive biomolecules for positron emission tomography imaging. *Theranostics* 2017; 7: 2924-2939.
- [16] Qin X, Guo X, Liu T, Li L, Zhou N, Ma X, Meng X, Liu J, Zhu H, Jia B and Yang Z. High in-vivo stability in preclinical and first-in-human experiments with [<sup>18</sup>F]AIF-RESCA-MIRC213: a <sup>18</sup>F-labeled nanobody as PET radiotracer for diagnosis of HER2-positive cancers. *Eur J Nucl Med Mol Imaging* 2023; 50: 302-313.

- [17] Feng Y, Sarrett SM, Meshaw RL, Vaidyanathan G, Cornejo MA, Zeglis BM and Zalutsky MR. Site-specific radiohalogenation of a HER2-targeted single-domain antibody fragment using a novel residualizing prosthetic agent. *J Med Chem* 2022; 65: 15358-15373.
- [18] Zhou Z, Vaidyanathan G, McDougald D, Kang CM, Balyasnikova I, Devoogdt N, Ta AN, McNaughton BR and Zalutsky MR. Fluorine-18 labeling of the HER2-targeting single-domain antibody 2Rs15d using a residualizing label and pre-clinical evaluation. *Mol Imaging Biol* 2017; 19: 867-877.
- [19] Zhou Z, Meshaw R, Zalutsky MR and Vaidyanathan G. Site-specific and residualizing linker for <sup>18</sup>F labeling with enhanced renal clearance: application to an anti-HER2 single-domain antibody fragment. *J Nucl Med* 2021; 62: 1624-1630.
- [20] Rinne SS, Dahlsson Leitao C, Gentry J, Mitran B, Abouzaied A, Tolmachev V, Ståhl S, Löfblom J and Orlova A. Increase in negative charge of <sup>68</sup>Ga/chelator complex reduces unspecific hepatic uptake but does not improve imaging properties of HER3-targeting antibody molecules. *Sci Rep* 2019; 9: 17710.
- [21] Jiang D, Lu X, Li Z, Rydberg N, Zuo C, Peng F, Hua F, Guan Y and Xie F. Increased vesicular monoamine transporter 2 (VMAT2) and dopamine transporter (DAT) expression in adolescent brain development: a longitudinal micro-PET/CT study in rodent. *Front Neurosci* 2019; 12: 1052.
- [22] Zhou Z, McDougald D, Meshaw R, Balyasnikova I, Zalutsky MR and Vaidyanathan G. Labeling single domain antibody fragments with <sup>18</sup>F using a novel residualizing prosthetic agent - N-succinimidyl 3-(1-(2-(2-(2-[(<sup>18</sup>F]fluoroethoxy)ethoxy)ethyl)-1H-1,2,3-triazol-4-yl)-5 (guanidinomethyl)benzoate. *Nucl Med Biol* 2021; 100-101: 24-35.